Progress Report on Model Development for Aerosol Transport through Divergent Cracks Paths

Spent Fuel and Waste Disposition

Prepared for US Department of Energy
Spent Fuel and Waste Science and Technology

Yadu Sasikumar
Oak Ridge National Laboratory

Jonah Lau, Stylianos Chatzidakis
Purdue University

September 30, 2023
ORNL/SPR-2023/3110
M4SF-23OR01020701

This report documents work performed under the Spent Fuel and Waste Disposition Campaign for the US Department of Energy Office of Nuclear Energy. This work was performed to fulfill the Level 3 milestone M3SF-20OR010207031 “Development and validation of phenomenological model on aerosol transport and plugging through stress corrosion cracks” within work package SF 20OR01020703 “Stress Corrosion Cracking - ORNL.”

SUMMARY

This report summarizes the progress in developing a phenomenological model of aerosol transport, deposition, and plugging through microchannels. The purpose of this effort is to introduce a user community—including researchers, regulators, and industry—to a generic, reliable numerical model for the prediction of aerosol transport while accounting for potential deposition and plugging of the leak paths to model spent nuclear fuel (SNF) release from postulated stress corrosion cracks in canisters under storage or transportation.

Current work is focused on expanding the model to predict aerosol (and gas) flow through complex microchannel (nozzle) geometries, in addition to the rectangular and cylindrical geometries as we approach more realistic stress corrosion crack conditions. In this regard, a divergent nozzle geometry used at Sandia National Laboratories (Sandia) for testing aerosol release and retention (Durbin et al. 2021), was added to the model. The model was then validated with blowdown data for the particular microchannel obtained from experiments conducted by Durbin et al. at Sandia. The report also presents preliminary non-benchmarked aerosol penetration fraction and mass flow rate for a monodisperse 10-micron (AED) particle concentration of 1.7e-08 kg/m^3 being released through the divergent microchannel geometry from the Sandia's aerosol experimental tank setup.

Future work will involve validating the aerosol model and updating the model's graphical user interface (GUI) to include the divergent nozzle geometry. This is expected to help stakeholders perform quick and easy first-principles calculations without the need to understand the underlying MATLAB script.

This report documents work performed under the Spent Fuel and Waste Science and Technology program for the US Department of Energy (DOE) Office of Nuclear Energy (NE). This work was performed to fulfil Level 4 Milestone M4SF-22OR010207012, "FY2022 Progress Report," within work package SF-22OR01020701.

This page is intentionally left blank.

ACKNOWLEDGMENTS

This research was sponsored by the Spent Fuel and Waste Science and Technology Program of the US Department of Energy and was carried out at Oak Ridge National Laboratory under contract DE-AC05-00OR22725 with UT-Battelle, LLC.

This report was developed with significant contributions, expert input, and guidance from Sam Durbin and Philip Jones at Sandia National Laboratories and Rose Montgomery at Oak Ridge National Laboratory.

This page is intentionally left blank.

CONTENTS

This page is intentionally left blank.

LIST OF FIGURES

This page is intentionally left blank.

ABBREVIATIONS

DOE	US Department of Energy
GDE	general dynamic equation
GUI	graphical user interface
NE	Office of Nuclear Energy
ORNL	Oak Ridge National Laboratory
SCC	stress corrosion cracking
SNF	spent nuclear fuel
Sandia	Sandia National Laboratories

This page is intentionally left blank.

1. INTRODUCTION

The current disposal pathway for commercial spent nuclear fuel (SNF) in the United States involves transfer from wet storage in pools to stainless-steel storage canisters for dry storage until a solution is finalized for ultimate disposal. The open volume between the canister and the surrounding shielding concrete cask allows passive ventilation from outside air which can impart dust and other contaminants that may collect on the outer surfaces of the canister. As the SNF sealed inside the canister cools, salts contained in the dust on the external canister surfaces may deliquesce to form concentrated brines, which under some conditions can evolve into stress corrosion cracks that could eventually penetrate through the canister wall. Of primary concern under such events is the potential release of radioactive aerosols from surface contamination, in-reactor failed fuel rods, or rods breached as a result of air ingress to the canister after canister breach (Durbin et al. 2021, Montgomery et al. 2022). Thus, understanding the aerosol transport and depressurization process of a postulated initiating event in an SNF canister is important for determining potential consequences as a result of stress corrosion cracking (SCC) formations (Chatzidakis 2021).

To expand the understanding of the processes occurring during the event and to extend the ability to predict released quantities, a generic numerical aerosol transport and plugging model that can predict the diffusion, deposition, and retention of aerosol particles in capillaries, slots, and cracks similar to stress corrosion cracks (Chatzidakis, 2018) is under development at Oak Ridge National Laboratory (ORNL) in collaboration with Purdue University (Chatzidakis and Sasikumar 2021; Chatzidakis and Scaglione 2019). This model could be used to improve the accuracy of consequence assessments, thus reducing the uncertainty of radiological consequence estimations by accounting for the filtering effect of leak path aerosol deposition and plugging in the source term.

This report highlights the addition of a divergent microchannel/nozzle geometry feature to the model. The microchannel is representative of the one used at Sandia for experimental testing (Durbin et al. 2021). This choice of geometry is the next step following testing of a simple slot orifice because it is more representative of the microchannel profile that results from the evolution of a stress corrosion crack. Section 2 of this report gives a brief background of the model and the underlying theory. Section 3 discusses the divergent nozzle geometry, its integration into the model, and additional features including the graphical user interface (GUI). Section 4 discusses the model's benchmarking against data from Sandia, and Section 5 summarizes the updated model and the future work scope with a brief overview of current efforts underway.

This page is intentionally left blank.

2. THEORY

The model in development is based on three sets of parameters describing (i) the thermodynamic behavior of the inert gas within the canister before, during, and after depressurization, (ii) the flow rate through a microchannel leak path, and (iii) the transport and deposition of aerosols within a microchannel leak path. It utilizes a theoretical approach (Williams 1994), assuming isothermal and 1D steady-state flow, allowing for the flow field to be determined and solved using respective continuity and momentum equations, as shown in the equations below:

Continuity: $$\rho_g A u = Q_m \quad (1)$$

Momentum: $$\rho_g u \frac{du}{dx} + \frac{dp}{dx} + 2\rho_g C_f \frac{v^2}{D_H} = 0 \quad (2)$$

Ideal gas law: $$p = \rho R_g T \quad (3)$$

Mass flow rate as a function of pressure drop along the flow direction derived from Eqs. (1) and (2):

$$p_u^2 - p_u^2 = R_g T Q_m^2 \int_0^L C_f(Re) \frac{\chi(x)}{A^3(x)} dx \quad (4)$$

For constant cross sections, Eq. (4) can be rewritten in a simplified form:

$$Q_m^2 = \frac{A^3(P_u^2 - P_d^2)}{\chi C_f L R_g T} \quad (5)$$

Reynolds number: $$Re = \frac{4Q_m}{\mu\chi}, \quad (6)$$

where C_f is the friction factor, R_g is the gas constant, p_u and p_d are the pressure at the upstream and at the downstream of the crack, respectively, T is the fluid temperature, L is the length of the duct, χ is the perimeter of the duct, and A is the cross-sectional area. A detailed derivation of the friction factors and flow equations can be found in the literature (Chatzidakis 2018).

Figure 1 shows a flowchart of the code and the different underlying steps involved in predicting penetration, retention, and modifications to a rectangular nozzle as a result of depressurization. The numerical solution first calculates the fluid velocity in each time step. Then the particle transport equation is solved using an implicit finite difference scheme. The duct radius is then updated through calculating the amount of the deposited mass. All the numerical integrations required in this calculation are performed using the trapezoidal rule (Chatzidakis 2020). The new cross section is then used for the aerosol calculations in the next step. In the original code, the iterative calculation for the Qm (volumetric flow rate) runs through the entire microchannel, which required adjustment to iteratively calculate Qm through each segment.

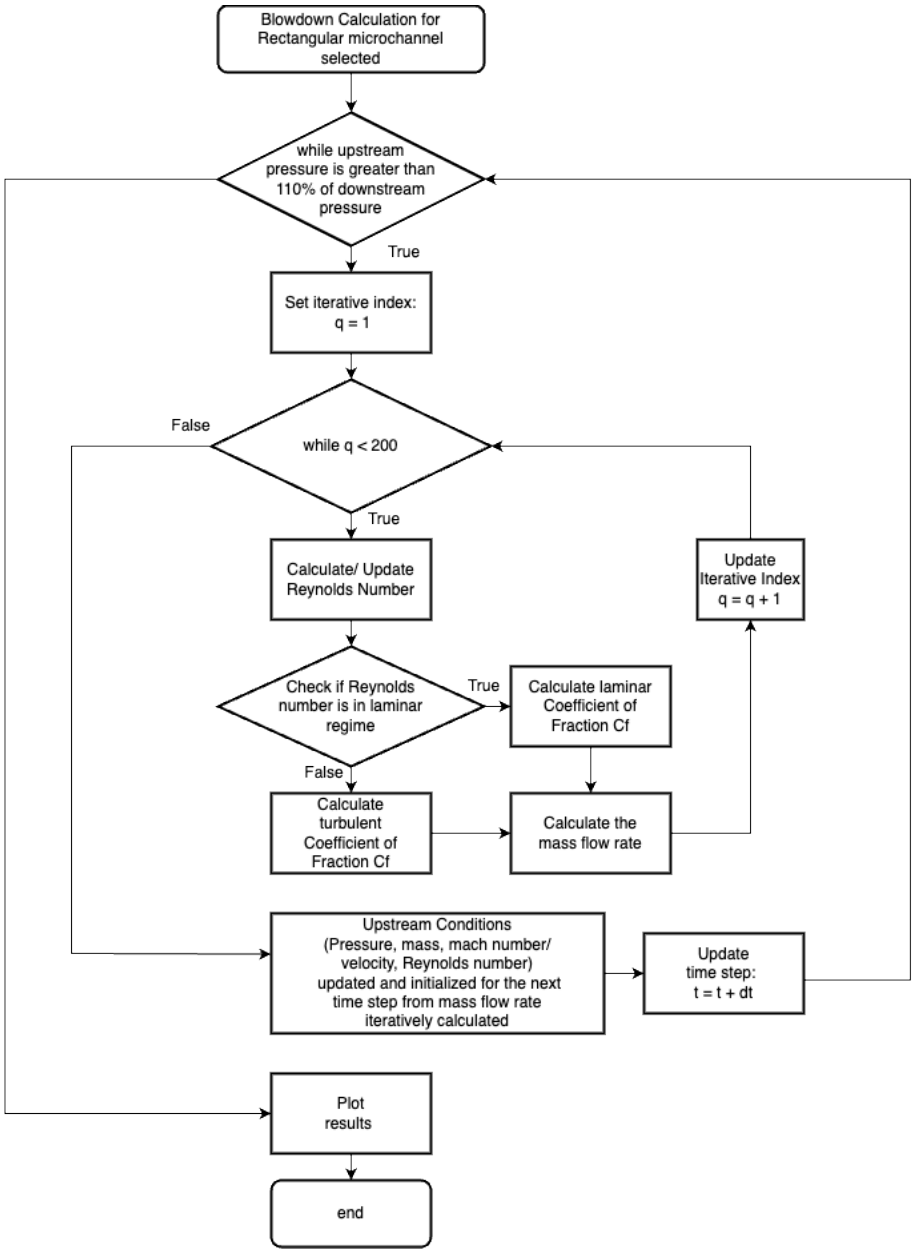

Figure 1. Flowchart for original blowdown model on rectangular microchannel.

An example of a single iterative blowdown calculation for a rectangular channel with length 0.00886 m, width: 28.9E-06 m and extent/height: 0.0127 m is as follows:

The input properties include:

Gas (air) properties:
Rg = 287 J/kg·k (gas constant)
T = 310 K (temperature)
μ = 1. 85E-05 Pa.s (dynamic viscosity)
γ = 1. 4 (specific heat ratio)

Initial conditions:
P(inlet) = 7. 48159E+05 Pa (initial inlet pressure)
P(outlet) = 1. 03421E+05 [Pa] (ambient/outlet pressure)
V = 0.908 m^3 (source volume)
Q_m = 0.0002 m^3/s (initial volumetric flow rate)

At the first iteration using Eqs. (5) and (6):

$$Re = \frac{4 \times 0.0002}{1.85 \times 10^{-5} \times 2 \times (0.0127 + 28.9 \times 10^{-6})} = 1698.63. \quad (7)$$

because Re < 2300,

$$C_f = \frac{24}{1698.63} = 0.0141. \quad (8)$$

Updated $Q_m = \sqrt{\frac{(28.9 \times 10^{-6} \times 0.0127)^3 \times \left((7.48159 \times 10^5)^2 - (1.03421 \times 10^5)^2\right)}{2 \times (28.9 \times 10^{-6} + 0.0127) \times 0.0141 \times 0.00886 \times 287 \times 310}} \cong 0.0003\ m^3/s$ (9)

This page is intentionally left blank.

3. PRELIMINARY MODEL OF THE DIVERGENT MIROCHANNEL/NOZZLE

As mentioned above, the divergent nozzle geometry that was added to the model is representative of that one used at Sandia for experimental testing (Durbin et al. 2021). The microchannel used by Durbin et al. has a slot opening that gradually increases in a linear fashion from 13 µm to 25 µm, with the 13 µm depth facing the upstream portion of the test section, as illustrated in Figure 2.

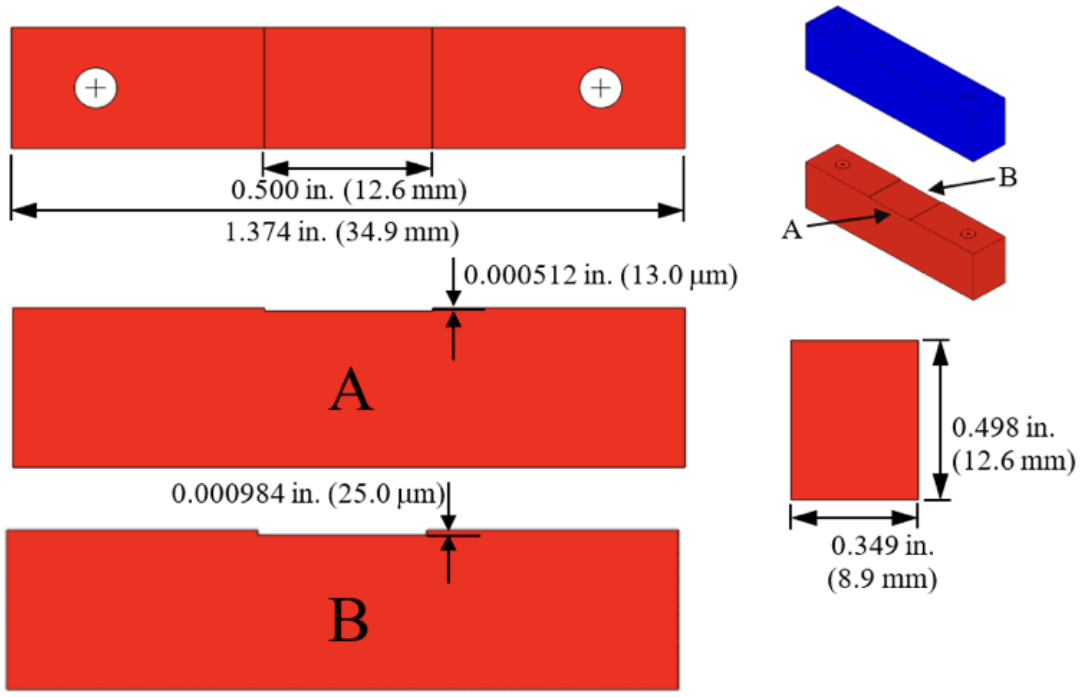

Figure 2. Sandia's linear block (13 to 25 µm depth transition) microchannel assembly (Durbin et al. 2021).

To characterize the flow through Sandia's linearly incremented slot opening using blowdown calculations in the original model (Chatzidakis 2018), it is assumed that a rectangular divergent nozzle represents the geometry used within the model. The divergent nozzle is divided into 200 segments that evenly distribute the nozzle's variable extent across an array of 200 cross-sectional extents (200-array discretization was chosen after numerous sensitivity trials) from 13 µm to 25 µm using the linspace function within MATLAB (Figure 3). At each segment (i = 1:200), the Qm (volumetric flow rate) is iteratively solved (200 iterations), resulting in characterization of flow for constant cross sections for each subsequent segment. The Qm at the last segment (i = 200, extent = 25 µm) is recorded for plotting, thus characterizing flow at the nozzle outlet/downstream.

As described in Section 2, the original blowdown model/MATLAB code (Chatzidakis 2018) for aerosol transport and microchannel applications only applied toward circular and rectangular cracks; hence, the code required tailoring to accommodate a rectangular divergent nozzle. To facilitate the accurate depiction and characterization of blowdown flow across the divergent nozzle, it was necessary to re-establish the length variable—which originally was the length of the entire rectangular or cylindrical channel—as the length of each segment. The width variable remained as a constant, in agreement with the slot nozzle microchannel assembly. With these geometric changes implemented, the model's blowdown calculation required modification to accommodate these changes. In the original code, the iterative

calculation for the Qm (volumetric flow rate) that runs through the entire microchannel required adjustment to iteratively calculate Qm through each segment.

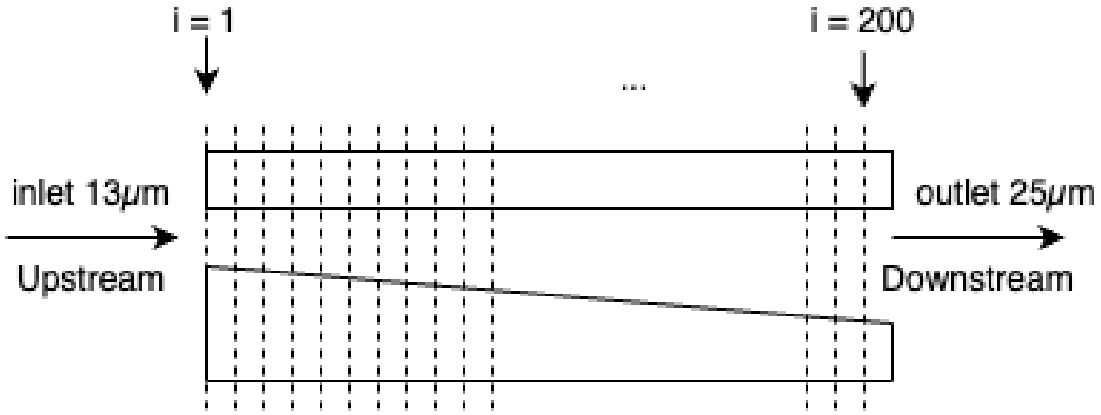

Figure 3. Divergent nozzle model to be implemented for blowdown calculation.

Based on the details above, Figure 4 presents a flowchart of the code and the different underlying steps required to predict the penetration, retention, and modifications to a nozzle that diverged as a result of depressurization.

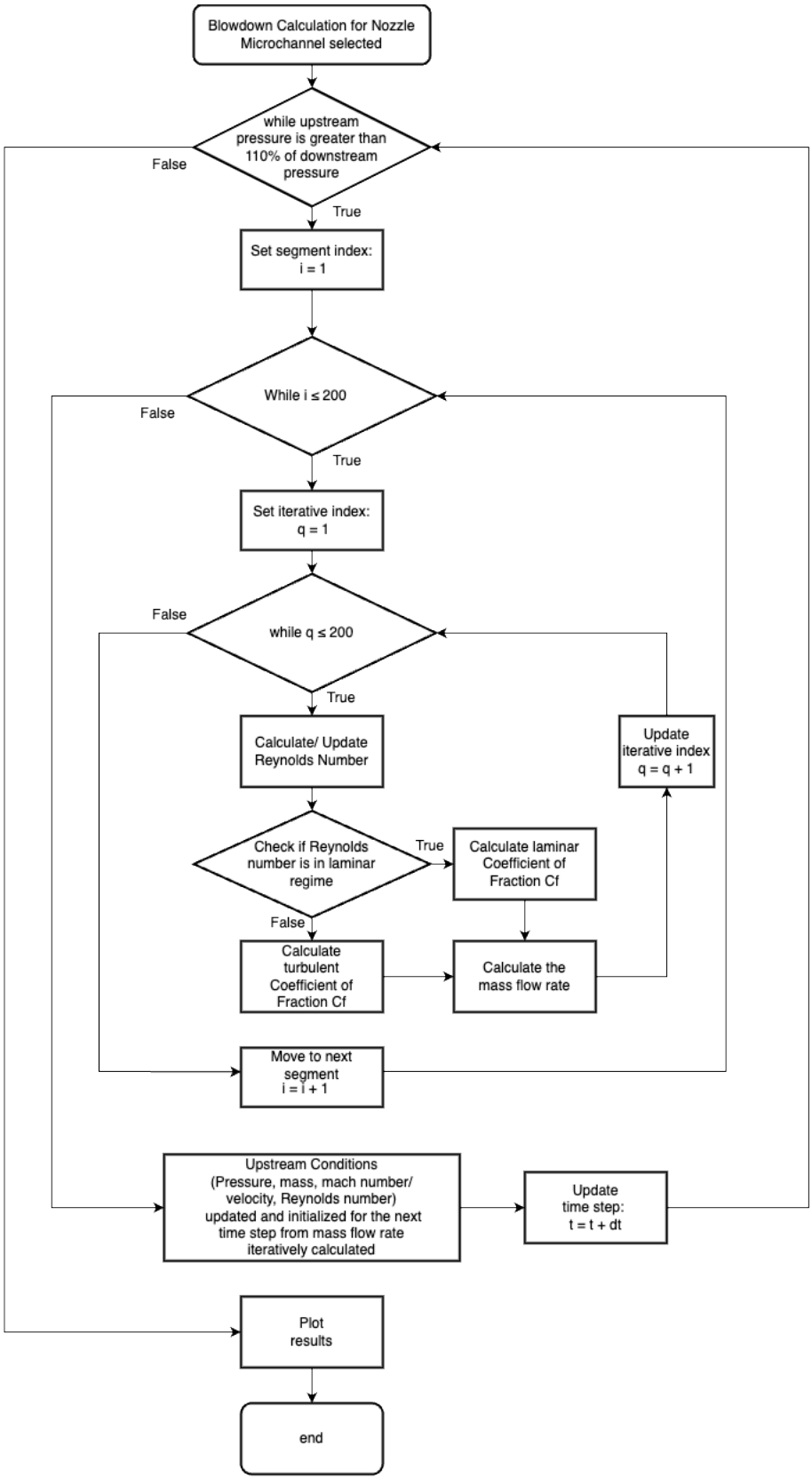

Figure 4. Flowchart for tailored blowdown model on divergent nozzle.

This page is intentionally left blank.

4. RESULTS AND BENCHMARKING

The updated model with the divergent nozzle was benchmarked with experimental blowdown data from Sandia. The flow results with air and helium are summarized in Figure 5, which shows the air mass flow rate through the clean microchannel (Figure 2) as a function of a wide range of pressure drops. The three initial pressure drops considered in the aerosol-laden tests are also shown for reference: nominally 120 kPa, 420 kPa, and 720 kPa, as indicated by solid diamonds in black, blue, and red, respectively. The velocity through the microchannel is roughly the same for both air and helium at the same pressure differential, but the mass flow rates are significantly different because of density.

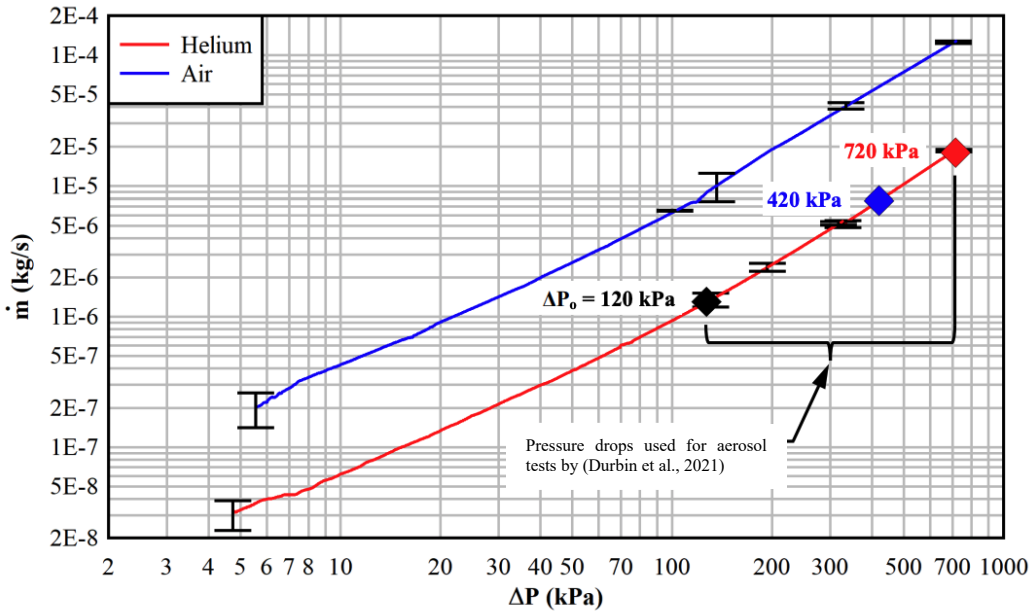

Figure 5. Experimental data (mass flow rate as a function of pressure drop across the linear microchannel (divergent nozzle) for helium (red line) and air (blue line).

Using a plot digitizer, data were obtained from the plots within Figure 5 for benchmarking the updated blowdown model, thus allowing for an accurate representation of flow through a divergent nozzle microchannel, as shown in the following section. Parameter tuning was applied on the friction factor Cf within the model to obtain the best fit because of the complexities of determining flow regimes in microchannels.

Figure 6 shows the output from the updated blowdown model benchmarked against experimental data for helium gas. It was found that through parameter tuning, the friction factor that provides the best representation of the experimental trends was $C_f = \frac{145}{Re}$ for laminar flow within a rectangular divergent nozzle microchannel. It was also ascertained from the benchmarked model that the flow regime remains within the laminar region for the duration of the blowdown procedure, as depicted in the plot of the Reynolds number vs. Time in Figure 7. Consequentially, this effort did not provide the opportunity for any parameter tuning methods to be applied toward the turbulent region for determining the friction factor. Based on analysis of Figure 6, it can also be stated that the model accurately fits the experimental trends within the pressure difference (ΔP) ranges of 30 kPa to 320 kPa.

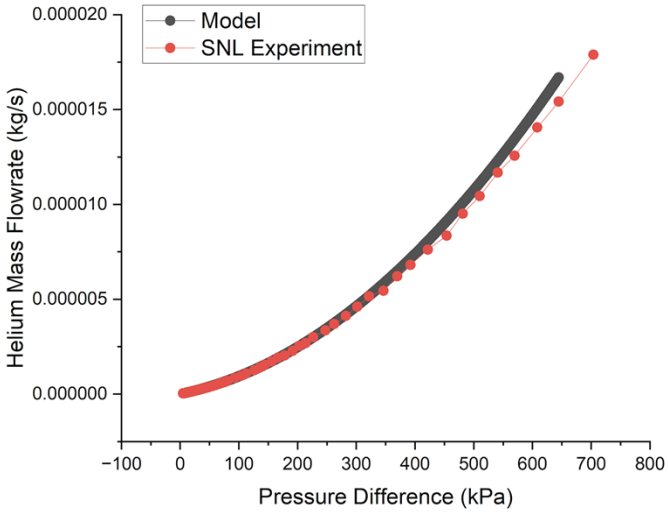

Figure 6. Updated blowdown model benchmarked against linear microchannel (divergent nozzle) data obtained from Sandia (helium gas).

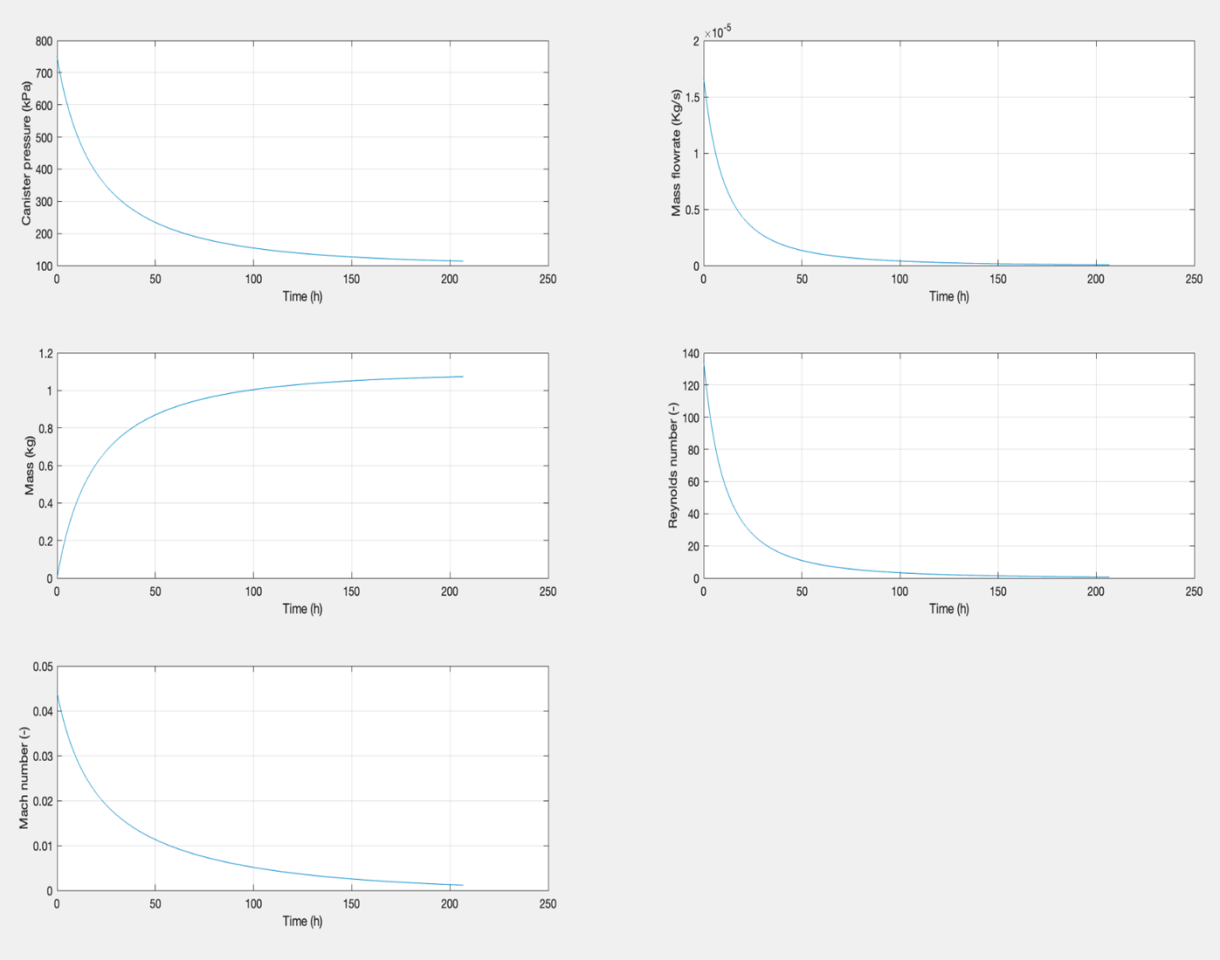

Figure 7. Time-dependent flow properties from updated blowdown model on divergent nozzle (helium gas).

Figure 8 shows the output from the updated blowdown model benchmarked against experimental data for air. In this case, parameter tuning indicated that the friction factor that provides the best representation of the experimental trends was $C_f = \frac{175}{Re}$ for laminar flow within a rectangular divergent nozzle microchannel. Like the helium gas blowdown calculations, the air blowdown did not reach turbulence regimes. Hence, the friction factor for the turbulent regime was not established. As seen in the case of helium, the model accurately fits the experimental trends within the pressure difference (ΔP) ranges of 10 kPa to 120 kPa before the experimental data diverge to only converge with the model at $\Delta P \simeq 600$ kPa. Figure 7 and Figure 9 show MATLAB output plots with the time-dependent flow properties of helium and air through the divergent nozzle. As expected, helium is seen to diffuse more quickly than air through the divergent microchannel.

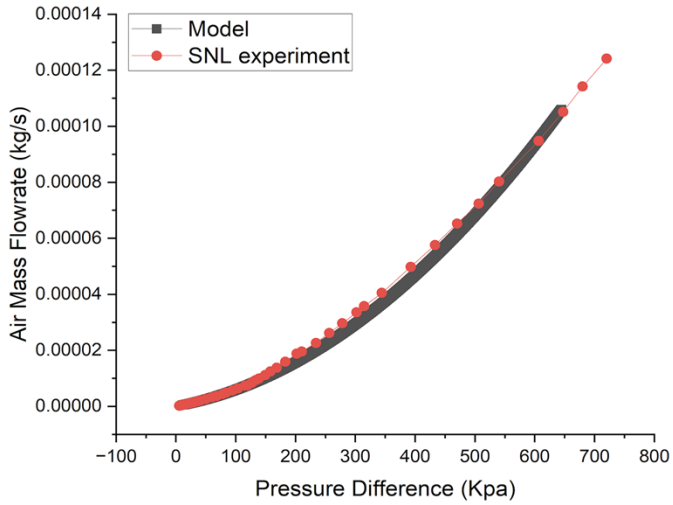

Figure 8. Updated BLOWDOWN MODEL benchmarked against linear microchannel (divergent nozzle) data obtained from Sandia (air).

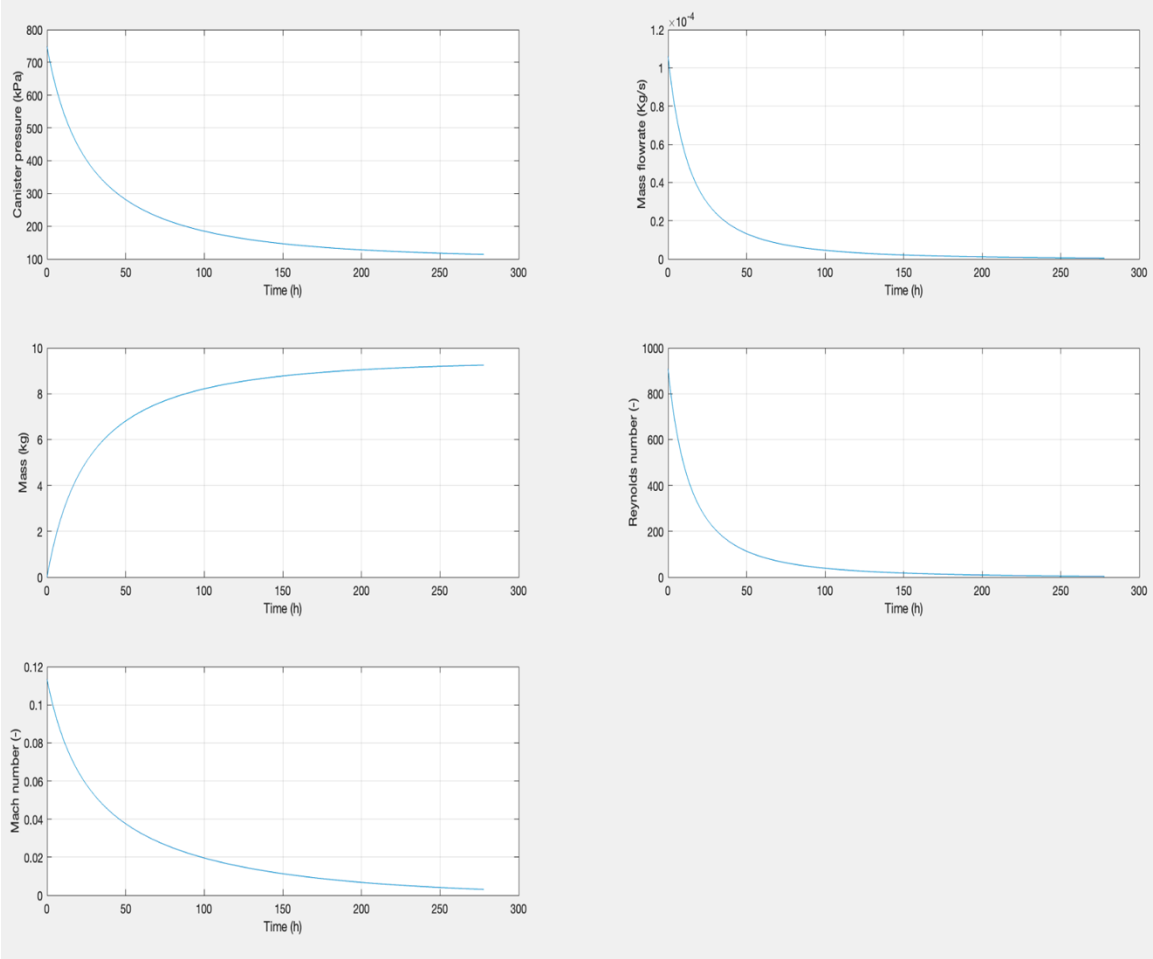

Figure 9. Time-dependent flow properties from updated blowdown model on divergent nozzle (air).

Finally, Figure 10 shows the preliminary model output plots for a monodisperse 10-micron (AED) particle concentration of 1.7e-08 kg/m^3 leaking through the divergent nozzle in the Sandia tank (Durbin et al. 2021), where an initial pressure of 748.159 kPa and a free volume of 0.908 m^3 was used. The figure shows the mass flow rate vs. the canister pressure and the penetration fraction vs. the velocity of the particle at 310 K. It is seen that the nozzle has a high penetration fraction for the velocities calculated ($\in$ [97.73%, 98.9868%]). The trends of the two plots agree with the general understanding and the previous results for rectangular and cylindrical geometries (Chatzidakis and Sasikumar, 2021). Benchmarking of the aerosol model with the divergent nozzle using results from Sandia experiments (Durbin, 2021) is currently underway.

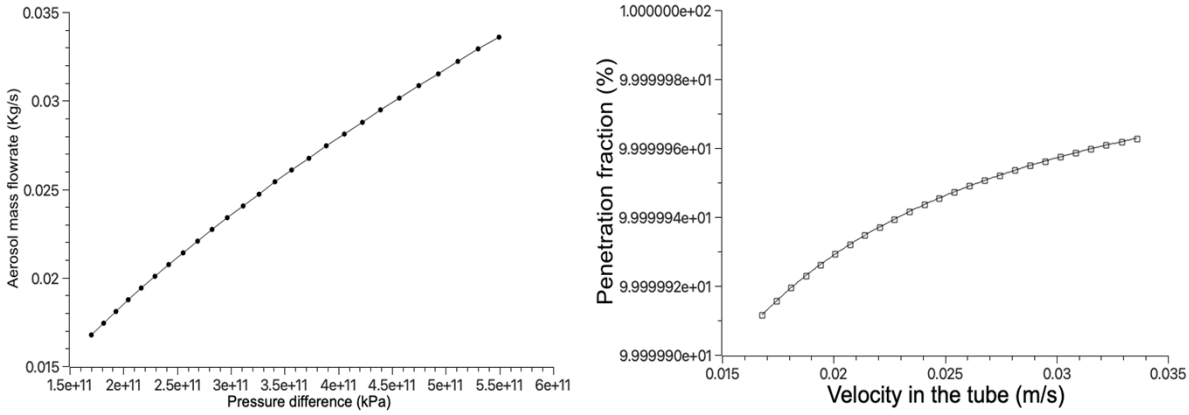

Figure 10. Pre-benchmarked aerosol transport results for the divergent nozzle using the Sandia tank initial conditions.

This page is intentionally left blank.

5. SUMMARY AND FUTURE WORKSCOPE

An updated numerical model for predicting the transport, deposition, and plugging of aerosols through linearly diverging microchannels is presented in this report. This updated model forms the next step in bridging the gap of accurately predicting radioactive aerosol transport through microchannels and microcapillaries that represent SNF contamination from postulated through wall stress corrosion cracks in canisters. The model has been benchmarked with experimental results from Sandia's testing results for air and helium blowdown through the divergent microchannel, showing good agreement. The model is currently being validated with aerosol laden blowdown experimental data from Sandia.

As mentioned in Section 4, the model could be improved with additional benchmark data, especially in the turbulent regime. The updated model could also be improved and optimized to allow for increased accuracy over larger ΔP ranges. This includes updating the geometry of the linear microchannel by further increasing the number of segments over which the iterative volumetric solving could take place, thereby increasing the accuracy of flow characterization over the microchannel. However, this however leads to the need for further optimization of the model within MATLAB.

Future work would also include implementing the divergent nozzle's geometry and the subsequent blowdown model within the "Aerosol Transport and Deposition in Spent Nuclear Fuel Dry Storage Casks" GUI developed by Dahm et al. (Dahm et al. 2022). Future research could also be performed to analyze application of the updated model to a divergence angle sensitivity test to characterize flow over a range of linear microchannels with different divergence angles. This leads to additional complex crack geometries that are more representative of SCC morphologies.

This page is intentionally left blank.

6. REFERENCES

Chatzidakis, S., and Sasikumar, Y. *Progress Report on Model Development for the Transport of Aerosol through Microchannels*, ORNL/SPR-2020/1599, Oak Ridge National Laboratory, Oak Ridge, Tennessee, April (2021).

Chatzidakis, S. *Progress Report on Model Development for the Transport of Aerosol through Microchannels* [Internet]. 2020. Available from: https://info.ornl.gov/sites/publications/Files/Pub143085.pdf

Chatzidakis, S., Scaglione, J. M. "A Mechanistic Description of Aerosol Transport and Deposition in Stress Corrosion Cracks." In: *Proceedings of Global/TopFuel 2019*. Seattle, Washington, United States of America: Global Top Fuel 2019; 2019. p. 1033–9.

Chatzidakis, S. *SCC Aerosol Transport Model Summary Report*. 2018 Dec 20 [cited 535 2022 Jun 29]; Available from: http://www.osti.gov/servlets/purl/1492159/.

Durbin, S., Pulido, R., Perales, A., Lindgren, E., Jones, P., Mendoza, H., et al. *Continued Investigations of Respirable Release Fractions for Stress Corrosion Crack-Like Geometries*. 2021 Jul 29 [cited 2022 Jun 28]; Available from: https://www.osti.gov/servlets/purl/1817839/.

Dahm, Z., Sasikumar, Y., Chatzidakis, S., Montgomery, R. "A Simple User Interface for Aerosol Transport and Deposition in Spent Nuclear Fuel Dry Storage Casks." In: *International High-Level Radioactive Waste Management Conference Proceedings* [Internet]. Phoenix: ANS; 2022 [cited 2023 Mar 2]. P. 208–11. Available from: https://www.ans.org/pubs/proceedings/article-52678/.

Montgomery, R., Sasikumar, Y,, Keever, T., Kumar, V. *Sister Rod Destructive Examinations (FY20) Appendix I: SNF Aerosols Released During Rod Fracture*. 2022 Mar 1 [cited 2022 May 16]; Available from: https://www.osti.gov/servlets/purl/1864438/.

Williams M. M. R. "Particle Deposition and Plugging in Tubes and Cracks (with Special Reference to Fission Product Retention)." *Prog. Nucl. Energy.* 1994 Jan 1;28(1):1–60.

This page is intentionally left blank.